Concept of scanning magnet with distributed winding coils for particle beam therapy

Takahiro Yamada,[1,*] Kazuya Nagashima,[1] Takuya Nomura,[2] Seiji Soeda,[2] and Noriaki Hino[1]

[1]*Hitachi, Ltd. Research & Development Group, 7-2-1, Omika-cho, Hitachi, Ibaraki, 319-1221 Japan*
[2]*Hitachi, Ltd. Smart Life Business Management Division, 2-1, Shintoyofuta, Kashiwa, Chiba, 277-0804 Japan*

(Received 20 September 2022; accepted 21 November 2022; published 14 December 2022)

To reduce the size of a rotating gantry for a particle therapy system, it is desirable to reduce the size of the scanning system by substituting separated scanning magnets with a combined-function scanning magnet. A two-dimensionally designed scanning magnet with distributed winding coils (DW-SCM) is proposed. The DW-SCM can generate a rotating dipole magnetic field using a single power supply. The two-dimensional static magnetic field distributions of the DW-SCM were calculated using POISSON SUPERFISH code and compared with those of an octupole scanning magnet (CW-SCM) and cos-theta-type scanning magnet (Cosθ-SCM) with the same bore diameter of 98 mm. The calculated two-dimensional magnetic field showed that the DW-SCM had the highest magnetic field strength of the three types of scanning magnets, and compared with the CW-SCM, the DW-SCM was 129% higher and the cos θ-SCM was 72% higher. The good field region (radius) of field homogeneity within $\pm 0.5\%$ of the DW-SCM had a symmetrical shape centered on a current phase of 30°, and the minimum value was 24 mm. Also compared with the CW-SCM, the minimum good field region was 11% higher for the DW-SCM and 65% higher for the cos θ-SCM. The results indicate that the proposed scanning magnet could generate a high-strength rotating dipole magnetic field, and it might be possible to reduce the size of a scanning system by substituting separated scanning magnets with the DW-SCM.

DOI: 10.1103/PhysRevAccelBeams.25.122402

I. INTRODUCTION

Particle beam therapy has recently become widespread for cancer treatment. Regarding irradiation techniques of particle beam therapy, the spot scanning technique [1–3] increases conformity to the target volume and modulates the dose more flexibly than the passive scattering technique. Spot scanning delivers the dose distribution as a set of discrete and narrow pencil beams such that the target volume is covered in Bragg peaks depending on the depth. To deliver a conformal 3D dose distribution, several thousand of such beams, each with different energies and positions, are required.

Most current scanning systems use two independent dipole magnets for transverse two-dimensional scanning [4]. The dipole magnets are arranged one after another on an irradiation nozzle located after a final bending magnet of a rotating gantry. The beam orbit scanned by the upstream magnet passes through the downstream magnet, which causes the scanning system to become large. To reduce the size of the gantry, it is desirable to reduce the size of the scanning system. This can be done by substituting the conventional magnets with a combined-function magnet capable of two-dimensional scanning.

Gordon *et al.* proposed an octupole scanning magnet that generates a rotating dipole magnetic field with the change in the loaded sinusoidal current phases [5,6]. This magnet consists of eight magnetic poles and eight coils concentratedly wound around the poles, and each pair of opposing coils is given a regular sinusoidal current provided by four independent power supplies. This octupole scanning magnet is referred to as the concentrated winding scanning magnet (CW-SCM). Similarly, a dodecapole magnet proposed by Brook can generate a rotating dipole magnetic field [7]. This magnet also has concentrated winding coils.

A cos-theta superconducting magnet is used to bend charged particles in high-energy accelerators [8]. In this magnet, the coils are arranged so that the magnetomotive force is distributed on a sinusoidal waveform with respect to the circumferential direction of the bore. By arranging

*Corresponding author.
takahiro.yamada.dp@hitachi.com

two cos-theta coils rotating 90° with respect to the beam direction, a scanning magnet capable of two-dimensional scanning can be constructed. Rotating the dipole magnetic field can be generated by exciting the two coils with two independent power supplies. This cos-theta scanning magnet is referred to as the cos θ-SCM.

We propose a new type of combined-function scanning magnet. The proposed magnet has distributed winding coils commonly used in electric motors and can generate a rotating dipole magnetic field. Conventional scanning magnets require multiple power supplies, but the proposed scanning magnet can be controlled by a single power supply. The proposed scanning magnet is referred to as the distributed winding SCM (DW-SCM). The purpose of this study was to evaluate the DW-SCM by comparing it with the above conventional scanning magnets.

II. MATERIALS AND METHODS

A. Concept of distributed winding scanning magnet

The DW-SCM uses a three-phase current to generate a dipole magnetic field in any direction, similar to the method of generating a rotating magnetic field in an electric motor. As shown in Fig. 1, the three-phase coils are arranged with a 120° shift. The exciting current is input to each coil with the intensity ratio of the three-phase alternating current whose phases are shifted by 120° according to (1). A dipole magnetic field is generated by combining the magnetic fields generated by each exciting current. The combined field is a pure cos θ field, and the field angle is determined by the current phase θ. With such an arrangement of exciting currents, two-dimensional scanning is possible by controlling the scanning direction (angle of scanning plane) by θ and the scanning angle by the current intensity I_0.

$$\begin{aligned} I_u &= I_0 \cos\theta \\ I_v &= I_0 \cos\left(\theta + \frac{2}{3}\pi\right) \\ I_w &= I_0 \cos\left(\theta + \frac{4}{3}\pi\right). \end{aligned} \tag{1}$$

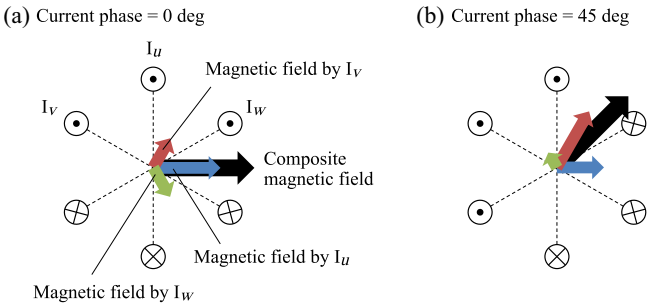

FIG. 1. Rotating magnetic field generated by DW-SCM (a) current phase $\theta = 0°$, (b) $\theta = 45°$.

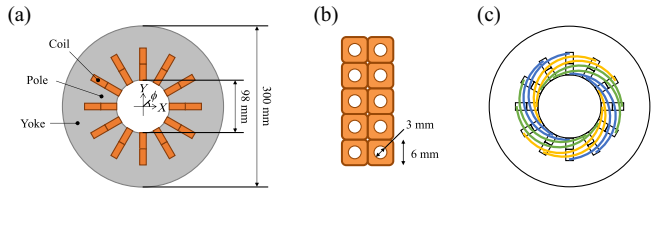

(d)

Coil angle ϕ [deg]	0	30	60	90	120	150	180	210	240	270	300	330
Inner coil	W1+	W2+	U1-	U2-	V1+	V2+	W3-	W4-	U3+	U4+	V3-	V4-
Outer coil	V2-	W3+	W4+	U3-	U4-	V3+	V4+	W1-	W2-	U1+	U2+	V1-

FIG. 2. Basic design of DW-SCM. (a) Cross-section of DW-SCM, (b) coil configuration, (c) coil connection at the coil-end region, (d) coil distribution table.

B. Two-dimensional design of DW-SCM

Figure 2 shows the configuration of the basic design of the DW-SCM. As shown in Fig. 2(a), 2 coils are arranged in each of the 12 slots surrounding the bore. The poles and yoke are composed of magnetic steel sheets laminated in the beam-traveling direction. Each coil consists of a six-turn hollow conductor [Fig. 2(b)]. The coil connection at the coil-end region and coil distributions in the slots are shown in Figs. 2(c) and 2(d). Each of the three-phase coils (I_u, I_v, and I_w) consists of four loops connected in series. For example, an inner coil with a coil angle of 0° forms a loop with an outer coil with a coil angle of 210°. The signs "+" and "−" in Fig. 2(c) indicate the direction of the current. From these coil distributions, the DW-SCM has a $5/6\pi$ short winding structure to improve the continuity of the magnetomotive-force distribution in the coil angular direction.

C. Comparison with conventional scanning magnets

To evaluate the physical characteristics of the DW-SCM, its two-dimensional magnetic field distributions were compared with those of the CW-SCM and the cos θ-SCM. The magnetic fields of the scanning magnets were computed using the POISSON SUPERFISH code [9]. Two-dimensional models of the scanning magnets are shown in Fig. 3. The cross-sectional shape of the CW-SCM was determined based on the scanning magnet reported by Jia *et al.* [6]. Based on the coil-arrangement method of a cosine-theta magnet [10], the cos θ-SCM has a shape in

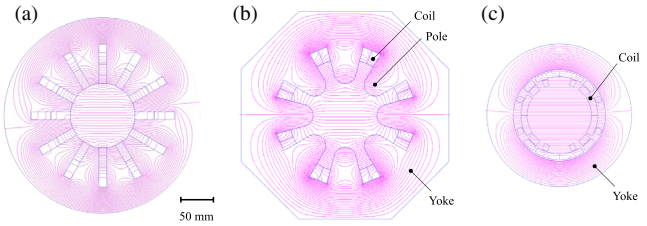

FIG. 3. Cross-section of SCMs: (a) DW-SCM, (b) CW-SCM, and (c) cos θ-SCM.

which three types of coils are arranged in one quadrant. To compare the field strength, the bore diameter, total magnetomotive force, and current density were unified to 49 mm, 40000 AT, and 28.8 A/mm^2, respectively, for all scanning magnets. The three magnets were compared regarding the field strength at the center and the good field region (GFR). The GFR was determined as a radius in which homogeneity of magnetic field vertical to a scanning plane was within ±0.5%. The homogeneity error size was determined so that the change in beam size (1σ) due to the scanning magnet would be 0.1 mm or less for a beam with the size of 6.0 mm at an isocenter. The beam size tolerance due to the scanning magnet was determined in consideration of the balance with the beam size variation caused by accelerators, such as during beam extraction. The beam size change was calculated by the following procedure: (i) The BL distribution of the integrated magnetic field along the particle trajectory of the outermost spot is calculated based on the two-dimensional magnetic field distribution. (ii) The quadrupole component of the BL distribution is calculated by a collinear approximation. (iii) The change in beam size (1σ) at the isocenter is obtained from a linear beam transport calculation with and without the quadrupole component.

To compare the scanning speed and the irradiation nozzle size, irradiation nozzles were designed for the three scanning magnets. In this comparison, the irradiation field size was unified to ϕ354 mm. Because the number of the required power supplies was different for the three magnets, the total power supply capacity was unified to keep the same power condition.

III. RESULTS

A. Magnetic field generated by DW-SCM

Figure 4 shows the distributions of magnetic flux lines and magnetomotive force of the DW-SCM at θ of 0°. As shown in Fig. 4(a), a dipole magnetic field was generated in the 0° direction. The magnetic field strength at the center was 0.444 T. As shown in Fig. 4(b), the magnetomotive force was distributed in a sinusoidal function with respect to the coil angle to generate the dipole magnetic field.

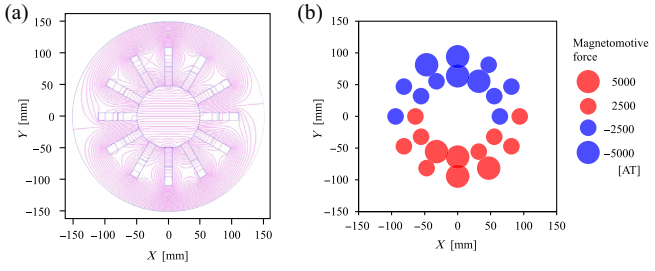

FIG. 4. Two-dimensional magnetic field calculation of DW-SCM, (a) magnetic flux line distributions, (b) magnetomotive force configuration at the current phase θ of 0°.

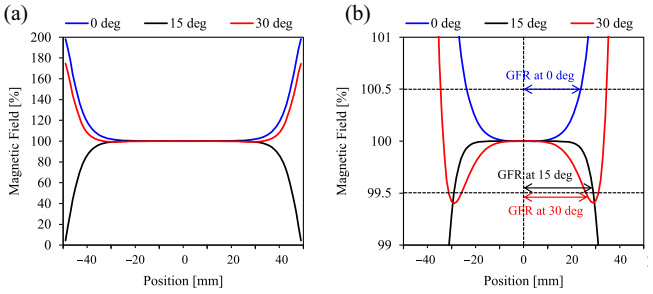

FIG. 5. Magnetic field transverse to scanning plane.

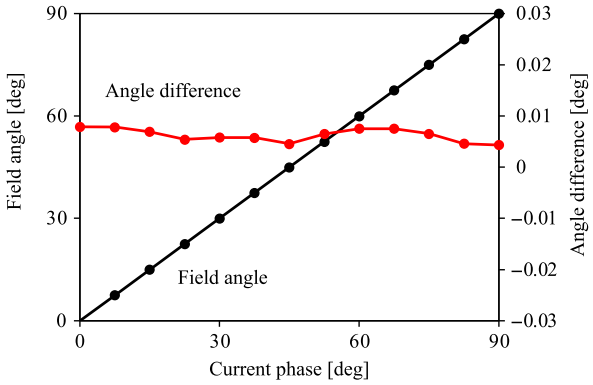

FIG. 6. Magnetic field angle with respect to θ.

Figure 5 shows the magnetic field strength vertical to the scanning plane with respect to θ. A flat magnetic field distribution was generated in every θ. The end magnetic field tended to be larger than the center at θ of 0 and 30° while it tended to be smaller than the center at 15°. The maximum difference between θ and the central magnetic field angle was about 0.01°, showing high linearity (Fig. 6).

B. Comparison with conventional scanning magnets

The field strengths at the center of the scanning magnets are shown in Table 1. The DW-SCM had the highest magnetic field strength of the three scanning magnets, and compared with the CW-SCM, the DW-SCM was 129% higher and the cos θ-SCM was 72% higher. As shown in Fig. 3, the CW-SCM had a lower magnetic field strength generated in the bore than the DW-SCM because a part of the magnetic flux passes between the adjacent magnetic poles rather than the bore. On the other hand, the DW-SCM generated a high magnetic field strength by arranging the coil close to the bore. In the cos θ-SCM, only the coils are

TABLE I. Field strength comparison.

Type	Field strength [T]
DW-SCM	0.444
CW-SCM	0.194
Cos θ-SCM	0.334

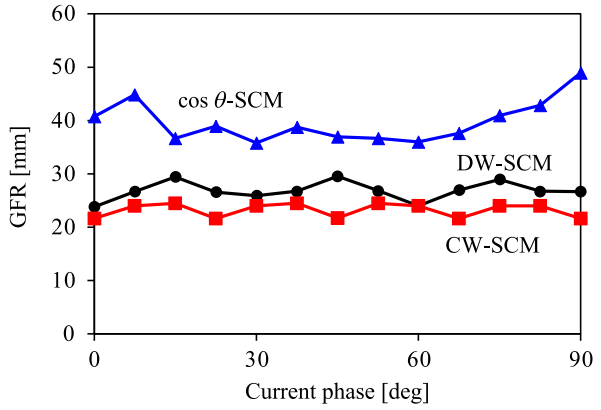

FIG. 7. Good field region (GFR) distributions of scanning magnets.

arranged outside the bore so that the coil region is the magnetic resistance. In the DW-SCM, however, the magnetic resistance was reduced and a high magnetic field strength was obtained by arranging the magnetic poles close to the bore.

The GFR distribution with respect to θ is shown in Fig. 7. The minimum GFR of the DW-SCM was 24.0 mm at θ of 0°. The GFR distribution of the DW-SCM reflected the symmetry of the magnetomotive force distribution so that the distribution had symmetry around 30°. Compared with the CW-SCM, the minimum GFR was 11% larger for the DW-SCM and 65% larger for the cos θ-SCM.

Table II shows the result of the nozzle design comparison. The source-axis distance of the DW-SCM was about as long as that of the cos θ-SCM. Compared with the CW-SCM, the scanning speed was 238% higher for the DW-SCM and 130% higher for the cos θ-SCM. As described later in the Discussions, the DW-SCM can be controlled by a single power supply. Because the total power supply capacity was unified in this comparison, the scan speed of the DW-SCM was faster than the others as a result of the increase in the exciting voltage due to the reduction in the number of power supplies. The scanning speed is 67.4 m/s when three power supplies of 500 A/600 V control the DW-SCM.

TABLE II. Magnet arrangements for proton therapy system.

Item	Unit	DW-SCM	CW-SCM	Cos θ-SCM
Source-axis distance	mm	1863	2917	1726
Pole length	mm	485	710	696
Kick angle	mrad	95.2	60.9	102.8
Field size	mm	ϕ354	ϕ354	ϕ354
Scan speed	m/s	38.9	11.5	26.4
Self-inductance	mH	2.56	2.71	3.47/4.05
Mutual inductance	mH	0.59	1.15	0
Maximum current	A	500	500	500
Maximum voltage	V	600	150	300
Power supply number	···	1	4	2

IV. DISCUSSIONS

We proposed a scanning magnet with distributed winding coils. By evaluating two-dimensional magnetic field distributions and comparing them with conventional scanning magnets, it was shown that the DW-SCM could generate a high-strength rotating magnetic field and a fast scan speed.

In the following, we discuss the power-supply configurations of the DW-SCM. Figure 8 shows the possible power-supply configurations. Conventional separated scanning magnets use two separated power supplies, as shown in Fig. 8(a). The CW-SCM requires four separated power supplies [5] and the cos θ-SCM requires two separated power supplies. The exciting current of the DW-SCM can be controlled by a single power supply, as shown in Fig. 8(b). Similar to a power supply of an electric motor, the pulse width modulation using an inverter makes it possible to control the current of the three coils independently. Although the specifications of the switching devices increase compared with the separated power supply, the size and cost of the power supply might be reduced by decreasing the number of switching devices and dc power sources. The three coils are connected in a star connection, as shown in Fig. 8(b). A delta connection can be used, but it is not suitable for a scanning magnet because excitation current instability might be caused by the recirculation in the three coils. Figure 9 shows a result of circuit simulation for an equivalent circuit in Fig. 8(b). Controlling target voltages for the pulse width modulation control as shown in Fig. 9(a), coil currents change linearly to a predetermined value.

An irradiation performance when using a single power supply and a magnet arrangement comparison with conventional separated scanning magnets [11] are shown in Table III. The source-axis distance is shortened by adopting the DW-SCM. The magnetic field strength can be increased by narrowing the bore diameter of the upstream side of the DW-SCM so that the pole length and the source-axis distance can be reduced.

In this comparison, the three coils of the DW-SCM are connected in a star connection so that their current is controlled by a single power supply. Scanning speed is reduced in Table III compared to Table II due to the reduction in the number of power supplies. Despite the

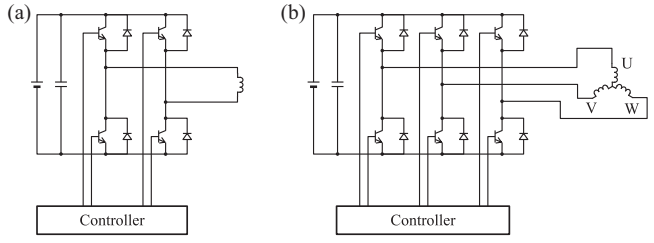

FIG. 8. Power-supply configurations: (a) separated power supply, (b) single power supply.

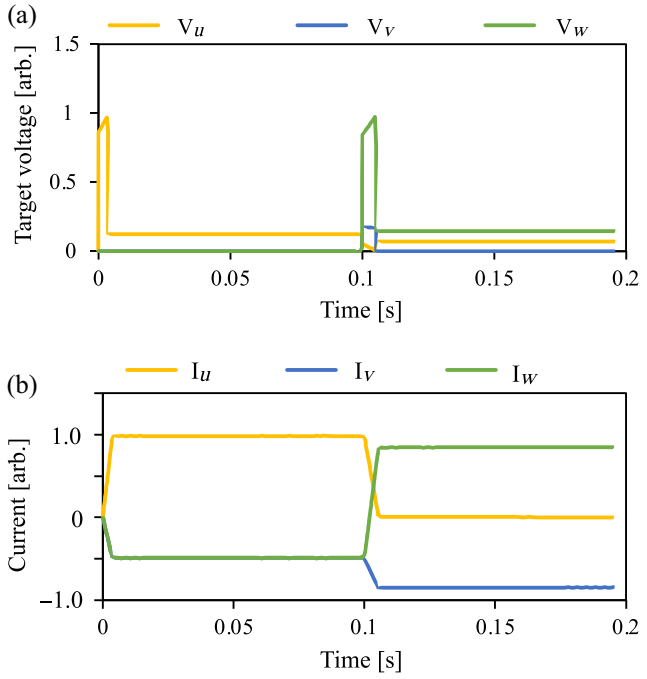

FIG. 9. Simulation of coil current control by a single power supply: (a) Target voltage for pulse width modulation control, (b) coil current.

small number of power supplies, the scanning speed of the DW-SCM is faster than that of the separated scanning magnets.

The two-dimensional magnetic field of the DW-SCM was evaluated in this study. It is necessary to evaluate the magnetic field distributions through three-dimensional simulations. It is also necessary to develop a power-supply control method based on inductance evaluation and to evaluate scanning performance based on particle-tracking calculation.

A three-dimensional design including the coil-end region is required for these simulations. In the coil-end region of the cos θ-SCM, the coil is arranged on a cylindrical surface, whereas in the DW-SCM, the coils can be arranged three dimensionally, so the axial length of the coil-end region might be shorter than that of the cos θ-SCM.

TABLE III. Comparison with conventional separated scanning magnets.

	Unit	DW-SCM	Separated
Source-axis distance	mm	1863	2300/2750
Pole length	mm	485	250/150
Field size	mm	ϕ354	300 × 300
Scan speed	m/s	38.9	9/20
Self-inductance	mH	2.56	20/14
Mutual inductance	mH	0.59	0
Maximum current	A	500	500/350
Maximum voltage	V	600	600/600
Power supply number	⋯	1	2

To apply the DW-SCM to a particle beam therapy system, high accuracy and stability of beam position and shape are required. To achieve high accuracy and stability, a correction method of current intensity and current phase according to the beam position might be necessary. A correction method might be also needed to reduce the effects of magnetic hysteresis that occur with the history of beam positions.

IV. CONCLUSIONS

We proposed a new type of scanning magnet that has distributed winding coils commonly used in electric motors. The proposed scanning magnet generates a rotating dipole using a single power supply. Magnetic field distributions were evaluated based on a two-dimensional model of the proposed magnet with a cross section of 12 slots and a $5/6\pi$ short winding structure. The magnetic field distributions were compared with those of conventional scanning magnets. The evaluation showed that the proposed scanning magnet could generate a high-strength rotating dipole magnetic field, and it might be possible to reduce the size of a scanning system by substituting separated scanning magnets with the proposed scanning magnet.

[1] Th. Haberer, W. Becher, D. Schardt, and G. Kraft, Magnetic scanning system for heavy ion therapy, Nucl. Instrum. Methods Phys. Res., Sect. A **330**, 296 (1993).
[2] E. Pedroni *et al.*, The 200-MeV proton therapy project at the Paul Scherrer Institute: Conceptual design and practical realization, Med. Phys. **22**, 1 (1995).
[3] T. Furukawa, T. Inaniwa, S. Sato, T. Tomitani, S. Minohara, K. Noda, and T. Kanai, Med. Phys. **34**, 1085 (2007).
[4] B. Jia *et al.*, The scanning magnets for proton therapy designed by SINAP, IEEE Trans. Appl. Supercond. **28**, 4400904 (2018).
[5] J. Gordon *et al.*, U.S. Patent No. 13 214 118 (2011).
[6] B. Jia *et al.*, Simulation of an octupole scanning magnet for spot scanning in proton therapy, IEEE Trans. Appl. Supercond. **28**, 4400304 (2018).
[7] S. J. Brooks, Configurable field magnets for a proton beam dynamics R&D ring, in *Proceedings of the 4th International Particle Accelerator Conference, IPAC-2013, Shanghai, China, 2013*, edited by Christine Petit-Jean-Genaz (JACoW, Shanghai, China, 2013), p. 3603.
[8] K. H. Mess *et al.*, *Superconducting Accelerator Magnets* (World Scientific, Singapore, 1996), p. 49–53.
[9] Los Alamos National Laboratory, POISSON SUPERFISH, available at http://laacg.lanl.gov/laacg/services/download_sf.phtml.
[10] CERN, Superconducting accelerator magnets. available at https://indico.cern.ch/event/683936/contributions/2803314/attachments/1564566/2689782/Schoerling_CASatEAS_2018.pdf.
[11] A. Smith *et al.*, The M. D. Anderson proton therapy system, Med. Phys. **36**, 9 (2009).